Journal of Cancer Science and Clinical Oncology
Volume 5 | Issue 1
ISSN: 2394-6520

Research Article Open Access

Degree of Malignancy of T-Cell Acute Lymphocytic Leukemia Related to Autofluorescence in an EL4-Based Model

Zhonghua Du[1], Lixia Wang[1], Yongguang Yang[1,2], and Yanping Yang[*1]

[1]Department of Hematology, First Bethune Hospital of Jilin University, Changchun, Jilin, China
[2]Columbia Center for Translational Immunology, Columbia University Medical Center, New York, USA

[*]**Corresponding author:** Yanping Yang, Department of Hematology, First Bethune Hospital of Jilin University, Changchun, Jilin, China, Tel:15804301706, E-mail: yangyanping_1978@163.com

Citation: Zhonghua Du, Lixia Wang, Yongguang Yang, Yanping Yang (2018) Degree of Malignancy of T-Cell Acute Lymphocytic Leukemia Related to Autofluorescence in an EL4-Based Model. J Cancer Sci Clin Oncol 5(1): 105

Received Date: June 01, 2018 **Accepted Date:** July 06, 2018 **Published Date:** July 09, 2018

Abstract

T cell acute lymphocytic leukemia (T-ALL) is an aggressive hematologic malignancy in terms of its pathology and populations. It is important to understand the phenomenon of autofluorescence in living cells because normal and cancer cells can be distinguished by this feature. However, the autofluorescence link to T-ALL is poorly understood. We provide direct evidence that EL4-based T-ALL model expresses both high autofluorescence ($FL1^+$) and low autofluorescence ($FL1^-$) in the current study. The $FL1^+$ phenotype is not as stable as the $FL1^-$ phenotype. Interestingly, $CD25^+$ cells of $FL1^+$ can transform to $CD25^+$ cells when injected into mice. Autofluorescence associated with differential expression of CD25 is related to the malignant degree of disease, which is presented by the tissue infiltration and growth speed of EL4 cells. Of note, the phenotypes of autofluorescence and CD25 expression of EL4 cells are related to the sensitivity to NK cells killing and the survival time of EL4-treated leukemic mice *in vivo*. Thus, autofluorescence monitoring might provide as new insight for investigating the malignant degree and prognosis index of T-ALL.

Keywords: Autofluorescence; T-ALL; CD25; Survival Term

Introduction

T-cell acute lymphoblastic leukemia (T-ALL) accounts for ~20% of acute lymphoma leukemias [1]. Patients usually exhibit hepatomegaly, splenomegaly and lymphadenectasis because of leukemic cell infiltration. In a number of non-hematopoietic and non-lymphatic tissues, such as endothelial cancers, including lung, breast, esophageal, skin, cervical and colorectal cancers, autofluorescence is abnormal in these neoplastic tissues; its imaging has also been used for the detection of precancerous lesions [2-5]. It is well known that autofluorescence is produced by living tissues or cells. As a safe, noninvasive, and rapid diagnostic strategy, autofluorescence detection is accepted by some institutions to research the function and phenotype of living cells [6]. Therefore, the purpose of our study was to research the characteristics of autofluorescence in T-ALL to improve strategies of management for this disease. Autofluorescence can distinguish between normal or malignant tissues; the same malignant tissue may differ according to its macroscopic type [7]. Fluorescence spectroscopy can detect the morphology and biochemistry of living cells, which are related to the metabolic activity, cellular proliferation and death of cells undergoing malignant changes. In neoplastic tissues, several factors result in reduced autofluorescence, such as decreased cytoplasmic ratio, loss of the submucosal collagen and increased hemoglobin concentration during neovascularization [8]. As a single-cell level, tumor endothelial cells present differing fluorescence compared with normal cells [9]. Impaired mitochondrial metabolism can change autofluorescence by mitochondrial NADH and FAD in cancer cells [10]. Excitation of mitochondrial NADH and FAD can result in cytoplasmic autofluorescence [11,12]. Dysplastic changes of cells can increase cytoplasmic autofluorescence by changing NADH and FAD levels [13]. Changes in cell physiology and pathology can alter the concentration of NADH [14]; NADH has been regarded as a biomarker for mitochondrial anomalies associated with cancer [15,16]. Relatively few studies on autofluorescence imaging and its mechanisms have been carried out; however, analyses of malignant hematopoietic and lymphatic tissues have been carried out more frequently than with endothelial cancers. It has been reported that leukocytes present autofluorescence [17]. In a lymphoma cell line, Chiaretti S *et al.* used autofluorescence to distinguish between normal and malignant cells [2]. Thus, it is necessary to further elucidate whether autofluorescence exists in T cell acute lymphocytic leukemia and lymphoma. We used EL4 cells, a T lymphoma leukemia cell line of mice, which can perfectly mimic the process

of T-ALL pathogenesis *in vivo* and represents a valuable cell culture model to study the biological characteristics of T-ALL. Firstly, we found that EL4 cells express $FL1^+$ and $FL1^-$ when injected into mice or cultured *in vitro*. Also, the $FL1^+$ phenotype is not as stable as that of $FL1^-$ cells. The expression of interleukin (IL)-2 receptor α chain (CD25) is strongly induced at the transcriptional level after T cell activation [18]. CD25 is a marker of activation of T cells; as EL4 cells are a T lymphoma leukemia cell line, it is needed to explore CD25 expression within such cells. Interestingly, $CD25^+FL1^+$ cells cultured *in vitro* transform to $CD25^-$ cells after the inoculation of mice; although $FL1^+$ and $FL1^-$ cells cannot transform into each other. We demonstrated that the differing growth speeds among different EL4 cell groups may be related to their expression of autofluorescence and CD25 (interleukin-2 receptor α; IL-2Rα). Furthermore, the EL4 groups with rapid growth speeds *in vitro* result in the short-term survival of mice when injected *in vivo*. These results may provide a cell biology-based insight into autofluorescence and its associated characteristics of T-ALL.

Materials and Methods

Cell Line and Cytotoxicity Assays

EL4 cell line (C57BL/6 origin) was obtained from the lab of the Translational Medicine Institution in Jilin University and was thawed from a frozen stock. Then was cultured on standard tissue culture plastic (12-well round-bottom plates) at an original concentration of 5×10^3 cells/mL and 1 mL/well in RPMI 1640 medium (Thermo Fisher Scientific) supplemented with 100 U/mL penicillin (Thermo Fisher Scientific), 10% fetal bovine serum (Thermo Fisher Scientific), 100 μg/mL streptomycin(Thermo Fisher Scientific), and 50 μmol/L 2-mercaptoethanol (Thermo Fisher Scientific), at 37 °C with 5% CO2. 1×10^6 cells/mL EL4 cells were cultured with or without 100 μl/mL IL-2 in 12-well-plates. We harvested EL4 cells and renovated complete medium every three days. On day 12, EL4 cells in each well were removed to culture on standard tissue culture plastic (6-well round-bottom plates) and 3mL/well in the same complete medium. EL4 cells were harvested and counted on day 14. EL4 cells were cultured with NK cells in a 4-hour chromium release assay as reported previously [19].

Mice

Wild-type (WT) C57BL/6 (B6) or C57BL/6(LY 5.2) mice were bred in pathogen-free conditions of the animal center affiliated to the First Bethune Hospital.

Flow Cytometry

Subsets of EL4 cells were stained with rat anti-mouse CD25-Allophycocyanin (APC). Propidium iodine (PI) staining was used to exclude dead cells. Rat anti-mouse FcγR mAb 2.4G2 was used to block non-specific FcγR binding. Antibodies were from BD Biosciences (San Diego, CA). Aliquots of 1×10^6 EL4 cells labeled with rat anti-mouse CD25-APC antibody were placed on ice for half an hour. After washing, we tested CD25 expression on FACS Canto™ II (BD Biosciences). In some experiments, $FL1^-$, $FL1^+25^+$, $FL1^+CD25^-$, $CD25^-$ EL4 cells were prepared by using the MACS system according to the manufacturer's instructions (Miltenyi Biotec) and cell sorting prior to injection into mice or culture *in vitro*. The purify (>99%) was tested by FACS.

Ethical Clearance

This research was performed according to the Care and Use of Laboratory Animals of the National Institutes of Health. The Ethical Review Boards of First Bethune Hospital of Jilin University approved this study (Protocol Number: 2017-004).

Statistical Analysis

Survival rate were analyzed using a Kaplan-Meier curve+logrank test with GraphPad Prism 5 (GraphPad Software, Inc. La Jolla, CA, USA). One-way ANOVA for multiple comparisons and unpaired student's t-test for two independent comparisons were used. Flow cytometric analyses were analyzed using FlowJo 10.0.7 software (BD FACSDivaTM software, New Jersey, USA). The statistical analysis was conducted using JMP13.0. Values indicate mean±standard deviation (SD). The data are presented as mean±SD. $P<0.05$ statistically significant.

Results

Distribution and Phenotype of EL4 Cells

To identify the biological characteristics of EL4 cells, including the distribution and their phenotype *in vivo*, original EL4 cells were recovered from liquid nitrogen and cultured for 7 days *in vitro*. WT B6 mice received EL4 cells and were then sacrificed when moribund. Vβ12 is the marker of EL4 cells and 100% EL4 cells were determined as Vβ12 positive ($V\beta12^+$) cells. As shown in Figure 1A, all EL4 cells expressing $V\beta12^+$ were distinguished from normal cells ($V\beta12^-$) by flow cytometry [20]. A total of $1x10^6$ EL4 cells were injected into naïve B6 mice-induced T-ALL mice. $V\beta12^+$ EL4 cells infiltrated every tissue, such as the spleen, bone marrow (BM), lymph nodes (LN), peripheral blood (PBMC), thymus, ovary, liver, lung (21.45±13.98%), and the kidney. The percentage of EL4 cells in every tissue was significantly different as determined by one-way ANOVA for multiple comparisons (*$P<0.05$). Especially in the liver, almost 57% EL4 cells were detected due to its percentage of nucleated

cells. Thus, EL4 cells harvested from the liver were used in the following experiments as the source of cells. We compared the phenotype of EL4 cells harvested *in vivo* and cultured *in vitro*. The same phenotype of CD3 on the surfaces of EL4 cells was seen *in vivo* and *in vitro*. As shown in Figure 1B, $FL1^+$ and $FL1^-$EL4 cells were detected; EL4 cells expressed CD3 both *in vivo* and *in vitro*. Interestingly, there was a different phenotype on the surfaces of EL4 cells. Although the expression of CD25 could be detected within FL1+ EL4 cells *in vitro*, no $FL1^+CD25^+$ cells were noted *in vivo* (Figure 1C). It is well known that CD25 expression can change during T cell activation. EL4 cells, as a T cell acute lymphoma leukemia cell line, were expected to show altered CD25 expression due to some unknown mechanisms. Thus, it was necessary to explore how $CD25^+$ cells change when injected *in vivo*. From the results above, we concluded that some phenotypes of $FL1^+$ EL4 cells were not as stable as that of $FL1^-$ EL4 cells, particularly CD25 expression. To determine the associated property of autofluorescence on EL4 cells, CD25 was employed as an important factor for investigation.

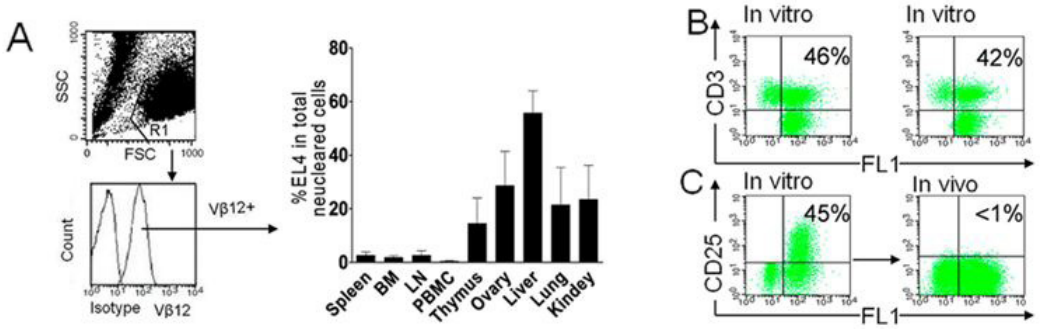

Figure 1: Distribution and Phenotype of EL4 cells. **A**. Left panel showed that all EL4 cells with $V\beta12^+$ were distinguished from normal cells with $V\beta12^-$ by flow cytometry. Naïve B6 mice (n=6) were injected i.v. with 1×10^6 EL4 cells. Right panel showed percentages (means±SD, n=8 per group) of $V\beta12^+$ EL4 cells in total neucleared cells in the indicated tissues when mice were moribund and assessed by flow cytometry two weeks later as following: spleen(2.58±1.32%), BM (1.84±0.66%), LN (2.56±1.77%), PBMC (0.41±0.22%), thymus (14.56±9.48%), ovary(28.62±12.88%), liver(56.77±8.29%), lung(21.45±13.98%), and kidney(23.47±12.81%). (*$p<0.05$). **B and C**. The normal cells types in the various tissues were $V\beta12^-$,while EL4 cells were $V\beta12^+$. Representative flow cytometry profiles showed the expression of CD3 and CD25 on original $V\beta12^+$ EL4 cells *in vitro* and *in vivo*. C. $CD25^+$ EL4 cells existed in original $FL1^+$ EL4 cells *in vitro* (left). No $CD25^+$ EL4 cells existed in $FL1^+$ EL4 cells *in vivo* (right)

Changes of Phenotype on EL4 Cells

To elucidate the phenotypic changes of $CD25^+$ cells *in vivo*, original EL4 cells were recovered from liquid nitrogen and cultured for 7 days *in vitro*. Cells were then separated into $FL1^+CD25^+$, $FL1^+CD25^-$, and $FL1^-$ cells by a MACS separation system. Then $A20^+$ C57BL/6(LY 5.2) mice received $1x10^6$ $A20^-FL1^+CD25^+$, $FL1^+CD25^-$ and $FL1^-$ EL4 subsets respectively. Two weeks later, mice were sacrificed when moribund. As normal cells were $FL1^-$ in B6 mice, we harvested $A20^-$ cells to observe changes in EL4 cells. The process of phenotype change was investigated when injected *in vivo* (Figure 2). $FL1^+CD25^-$ EL4 cells harvested from the livers of mice may originate from $FL1^+CD25^+$ cells in vitro as there were no $FL1^+CD25^-$ cells *in vivo* (Figure 2A). In

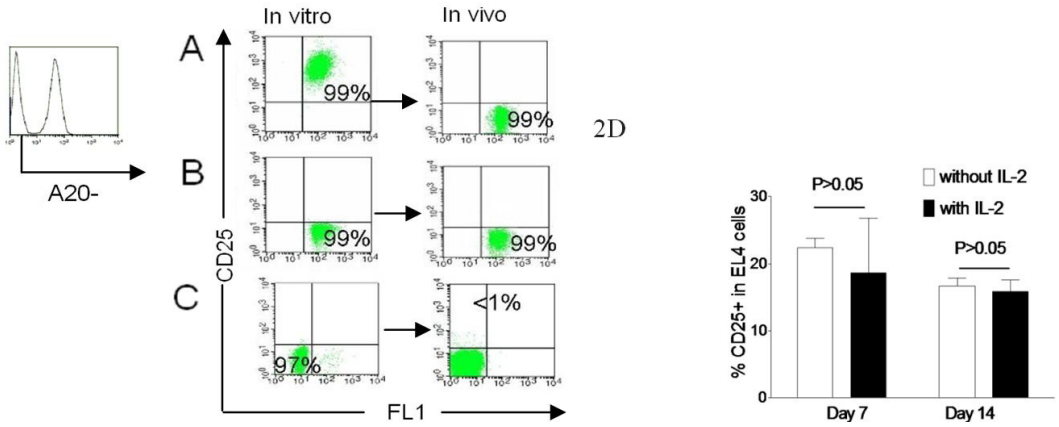

Figure 2: Changes of phenotype on EL4 cells. Representative flow cytometry profiles showed the expression of CD25 on EL4 cells *in vitro* and *in vivo*. Original EL4 cells were recovered from liquid nitrogen and cultured 7 days in vitro, then these cells were separated into $FL1^+CD25^+$, $FL1^+CD25^-$ and $FL1^-$ cells with anti-CD25 microbeads followed by positive or negative selection using the MACS separation system. The 1×10^6 EL4 cells were injected into C57BL/6(LY 5.2) mice respectively. C57BL/6(LY 5.2) mice expressing $A20^+$ were received $A20^-$ EL4 cells for the sake of discrimination $FL1^-$ EL4 cells and normal cells. Mice with EL4 cells were sacrificed when moribund two weeks later. **A**. $CD25^+$ EL4 cells transformed to $CD25^-$ EL4 cells *in vivo*. **B and C**. No phenotype change of $CD25^-$ EL4 blasts *in vivo*. **D**. Comparison of percentages of CD25 expression with IL-2. EL4 cells without IL-2 (left) and EL4 cells with IL-2 (right) were prepared as above and were cultured with or without 100 μl/mL IL-2 at an original concentration of 1×10^6 cells/mL in 12-well-plates. Cultures were set up in three replicates each. Shown are percentages (means±SD) of $CD25^+$ cells in EL4 cells on day 7 or day 14 by flow cytometry. Data represented the average of triplicate samples. There were no significant differences between groups with or without IL-2

addition, no FL1$^+$CD25$^-$ cells *in vitro* transformed into FL1$^-$CD25$^-$ cells in vivo (Figure 2B). Furthermore, FL1$^-$ cells *in vitro* could not transform into FL1$^+$ cells; CD25$^-$ cells *in vitro* could not transform into CD25$^+$ cells *in vivo* (Figure 2C). These results indicated that FL1$^+$ and FL1$^-$ EL4 cells cannot transform into each other; however, CD25$^+$ cells were found to transform into CD25$^-$ cells. Therefore, no CD25$^+$ EL4 cells were seen *in vivo*. It was suggested that the expression of CD25 is in proportion to the FL1$^+$ phenotype of EL4 cells. We also aimed to study the factors that affect the expression of CD25. IL-2 is known to induce CD25 expression on activated T cells. In our study, however, no changes in CD25 expression were seen when EL4 cells were cultured with or without IL-2 at day 7 or 14 (Figure 2D). Therefore, it is possible that there are other factors that regulate the expression of CD25 on EL4 cells. Although mechanisms remain unclear, our study shows that changes in CD25 expression may independent of IL-2.

Characteristics of Different Phenotypes of EL4 Cells

To further test whether there were differences in the biological characteristics of CD25$^+$ or CD25$^-$ EL4 cells, WT B6 mice were injected the same number of CD25$^+$ or CD25$^-$ EL4 cells (1x106), and were sacrificed 2 weeks later. We found that there were differences in the sizes of liver infiltrated by EL4 cells. Hepatomegaly was markedly severe in mice injected with CD25$^-$ EL4 cells than those injected with CD25$^+$ EL4 cells (Figure 3A). The average liver weight between CD25$^+$ and CD25$^-$ EL4-treated mice is significantly different (1.763±0.072 g vs. 1.458±0.076 g) (n=5 per group, mean ± SD, P<0.05). Therefore, it is necessary to further demonstrate whether there is a disparity of survival term between these two groups of mice due to the notable degree of tissue infiltration of EL4 cells. As shown in Figure 3B, WT B6 mice received the same number of CD25+ or CD25$^-$ EL4 cells (5x10); the survival term was significantly reduced in mice injected with CD25$^-$ cells than CD25$^+$ cells (P<0.01). These results demonstrated that CD25$^-$ EL4 cells induced notably severe hepatomegaly and short survival term compared with CD25+ EL4 cells. Therefore, it is likely that CD25$^-$ EL4 cells are more malignant, leading to rapid disease progression. Furthermore, an NK cell cytotoxicity assay was performed with CD25$^+$ and CD25$^-$ EL4 cells. The result showed that CD25$^+$ EL4 cells were more sensitive to NK cells (Figure 3C). Therefore, it is possible that the decreased malignancy of CD25$^+$ EL4 cells may be attributed to NK cell killing. Another possibility is that the transformation of CD25$^+$ EL4 cells may affect the degree of malignancy. As

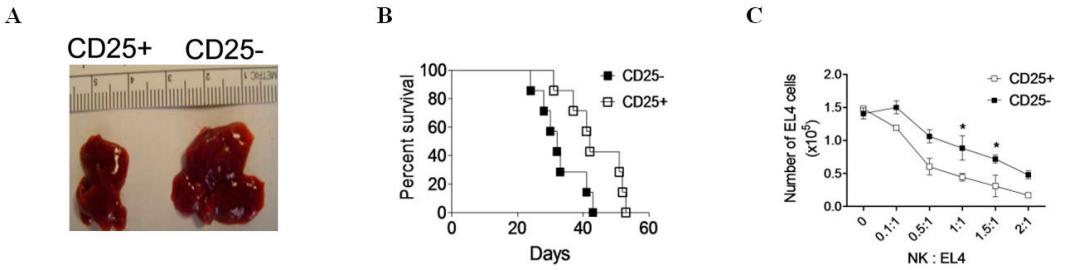

Figure 3: Characteristics of CD25 expression on EL4 cells. **A-C**. CD25$^+$ and CD25$^-$ EL4 cells were prepared as above. **A**. Mice with CD25$^+$ and CD25$^-$ EL4 cells were moribund and sacrificed two weeks later. Representative Hepatomegaly was observed much more severe in mice injected with CD25$^-$ EL4 cells than mice with CD25$^+$ EL4 cells. **B**. WT B6 mice were injected with 5×104 CD25$^+$ (□) or CD25$^-$ (■) EL4 cells respectively. The difference of survival curves of CD25$^+$ or CD25$^-$ recipients was statistically significant (p=0.01) (n=7 per group). **C**. CD25$^+$ EL4 cells were more sensitive to NK cells cytotoxicity (n=5, *p<0.05)

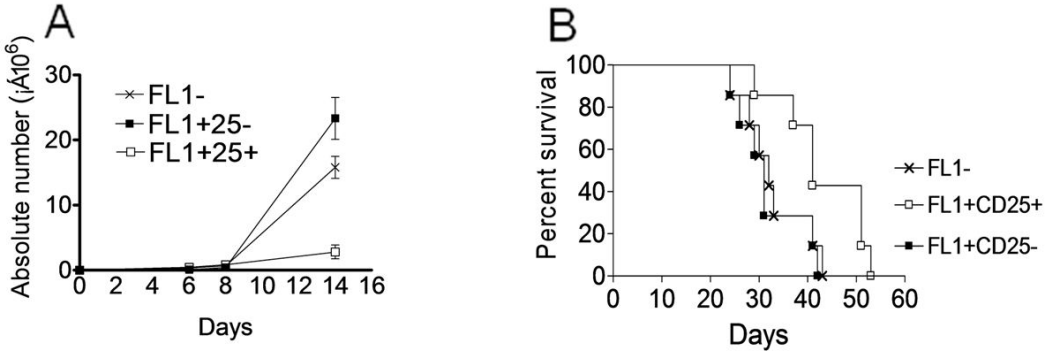

Figure 4: A. Comparison of growth curves of different phenotypes of EL4 cells. FL1$^-$ EL4 cells (×), FL1$^+$CD25$^+$ EL4 cells (□), or FL1$^+$CD25$^-$ EL4 cells (■) were prepared by MACS as above. Every group was cultured in 12-well-plate at an original concentration of 5×103 cells/mL for 14 days and every line represented every group. Absolute number of EL4 cells was indicated by growth curve. In comparison with FL1$^+$CD25$^+$ EL4 cells, FL1$^-$ and FL1$^+$CD25$^-$ EL4 cells showed significantly quickly growth speed (n=7 per group, p=0.013, p=0.004 respectively). The similar growth speed was observed between FL1$^-$ and FL1$^+$CD25$^-$ EL4 cells. Data represented the average of triplicate samples and results were expressed as Means±SDs. B: Comparison of survival term of different phenotypes of EL4 cells. The same number of 5×10^4 EL4 cells in every phenotype were injected into WT B6 mice including FL1$^-$ EL4 cells (×), FL1$^+$CD25$^+$ EL4 cells (□), or FL1$^+$CD25$^-$ EL4 cells (■) and survival term was shown. In comparison with FL1$^+$CD25$^+$ EL4 mice, FL1$^-$ and FL1$^+$CD25$^-$ EL4 cells showed significantly short survival term (p=0.040, p=0.037 respectively) (n=7 per group). The similar survival term was observed between FL1$^-$ and FL1$^+$CD25$^-$ EL4 cells. The median time to death was (×) 32days, (■) 31days and (□) 41days. Results shown were representative of three independent experiments

there were differing degrees of disease progression induced by EL4 cells according to their expression of CD25, we investigated whether there were differences in growth speed between $CD25^+$ and $CD25^-$ EL4 cells. Since no expression of CD25 in $FL1^-$EL4 cells was detected, EL4 cells were separated into $FL1^+CD25^+$, FL1+$CD25^-$ and $FL1^-$ populations by a MACS separation system. We found that FL1+CD25+ EL4 cells grew significantly slower than FL1+$CD25^-$ EL4 (P=0.004) and $FL1^-$ EL4 cells (P=0.013) (Figure 4A). Similar growth speeds were seen between $FL1^+CD25^-$ and $FL1^-$ cells. Then, we continued to test the hypothesis that the mortality of mice treated with various EL4 cell groups differs according to their phenotype in vivo. So, $5x10^4$ $FL1^-$, $FL1^+CD25^+$ and $FL1^+CD25^-$ EL4 cells were respectively injected into naïve B6 mice. The survival time of $FL1^+CD25^+$ EL4-treated mice was longer than that of $FL1^+CD25^-$ $EL4^-$ and $FL1^-$ EL4-treated mice. As shown in Figure 4B, the difference in mortality of mice was statistically significant for the $FL1^+CD25^+$ EL4-treated mice versus the $FL1^-$ EL4-treated mice (P=0.04), and the $FL1^+CD25^+$ EL4-treated mice versus $FL1^+CD25^-$ EL4-treated mice (P=0.037). Taken together, these results demonstrated that $FL1^+CD25^+$ EL4 cells induced slow progression of disease, which was presented as slow growth speed *in vitro* and long survival term *in vivo*.

Discussion

The illumination of unstained cells that naturally emit light is termed as autofluorescence. It is important to understand phenomenon of autofluorescence in living cells as this distinguishes normal and cancer cells. For many endothelial tissues, dysplastic changes result in increased contents of mitochondrial NADH and FAD, which leads to changes in autofluorescence in cancer [13]. For diseases of malignant hematopoietic and lymphatic tissues, a previous report showed that autofluorescence can distinguish between a type of malignant B cell and normal lymphocytes [2]; however, the characteristics of autofluorescence in T cells lymphoma leukemia remains unknown. T cell acute lymphoma leukemia is characterized as a heterogeneous disease with poor prognosis [21]. By using an EL4-based T-ALL model, to the best of our knowledge, we first reported that these cells express $FL1^+$ and $FL1^-$ both *in vivo* and *in vitro*. $CD25^+$ EL4 cells only persisted in $FL1^+$ populations *in vitro* as they are observed to transform to $CD25^-$ cells following injection into mice. It is possible that the transformation may require time as $CD25^+$ cells induce notably longer terms of survival compared with $CD25^-$cells *in vivo*. Another possibility is that $CD25^+$ EL4 cells are more sensitive to NK cell cytotoxicity. Furthermore, notable severe tissue infiltration, such as hepatomegaly, appears in mice with $CD25^-$ cells when the same numbers of $CD25^+$ or $CD25^-$ EL4 cells are injected at the same time. These results indicate that the expression of CD25 in $FL1^+$ might be related to the degree of malignancy of T-ALL in an EL4 model. This was further determined by separating EL4 cells into $FL1^+CD25^+$, $FL1^+CD25^-$ and $FL1^-$ populations. We observed that $FL1^+CD25^+$ cells grow more slowly than $FL1^+CD25^-$ and $FL1^-$ cells, which was statistically significant as determined with growth curves. Additionally, $FL1^+CD25^+$ cells result in statistically significant long-term survival compared with $FL1^+CD25^-$ and $FL1^-$ cells. The survival term of $FL1^+CD25^-$ and $FL1^-$ cells is similar without statistical significance. Autofluorescence was associated with expression of CD25 and may therefore be related to tissue infiltration, speed of growth and survival term in the EL4-based T-ALL model in the current study.

Over the past few decades, autofluorescence analysis is regarded as a promising way to distinguish between normal and cancer cells. The diagnostic applications of this method has notably increased [22]. The characteristics of autofluorescence in tissues are determined by the morphological and biochemical states of cells [23]. Malignant tissues and the corresponding normal tissues can be distinguished by autofluorescence [24]. Regarding the autofluorescence of malignant lymphatic tissues, a study reported that the fluorescence of lymphoma is significantly lower than that of lymphoid hyperplasia and normal tissues. It has also been shown that the accuracy is 91.5% by the visual classification of autofluorescence imaging (AFI). Thus, AFI may be regarded as a useful tool to indicate the disease stage and appropriate therapy in the certain types of lymphoma [25]. Furthermore, autofluorescence has been observed in leukocytes, such as macrophages, eosinophils and neutrophils [26]. Our data indicates that autofluorescence appears in an EL4-based T-ALL model; investigation of its characteristics might have clinical value for patients with T-ALL. CD25 is termed as the interleukin-2 receptor α chain, which is expressed on the surfaces of activated T cells and a type of T cell lymphoma leukemia, known as adult T-cell leukemia [27]. In our study, we reported that EL4 cells, as a model of T-ALL, partially express CD25 *in vitro*. We also demonstrated that $CD25^+$ cells are not detected *in vivo* because they transform into $CD25^-$ cells. Since both the expression and transformation of CD25 appear with high autofluorescence of EL4 cells, these data raise a possibility that high autofluorescence might not be as stable as low autofluorescence. Furthermore, different phenotypes associated with autofluorescence result in varying extents of tissues infiltration, growth speed and survival term. This may be consistent with the findings of the current study in which cell autofluorescence was related to the degree of cell differentiation. It has been identified that autofluorescence decreased when cells differentiate [28]. Until recently, the biological knowledge of T-ALL was limited [29]. Thus, autofluorescence monitoring might provide new insight into the processes of differentiation, which may further contribute to investigations into the malignant degree and prognosis index of T-ALL. However, a limitation of the present study is that we did not analyze clinical samples of T-ALL patients; we lacked clinical data to further identify our results. In the future, we will collect peripheral blood samples of T-ALL patients to investigate the expression CD25 and in relation to autofluorescence. In conclusion this new finding that autofluorescence exists in EL4-based T-ALL cells provides an insight into hematologic malignancies and lymphoma disease. Although cells with different autofluorescence intensities cannot transform into each other from in vitro to *in vivo*, its stability is not coincident such as different expression of CD3, CD25, and TCRαβ only existed in $FL1^+$ EL4 cells. The expression of CD25 can transform

in $FL1^+$ cells as seen *in vitro* and *in vivo*, and is related to growth speed and survival term. Although no exact mechanisms have been clarified, our study shows that T-ALL, at least in the EL4 model, may present varying intensities of autofluorescence. This application of this approach showed that the expression of CD25 in $FL1^+$ cells is related to the degree of malignancy of T-ALL, which may facilitate future mechanistic studies. Therefore, autofluorescence combined with CD25 expression may be considered as a useful adjunctive diagnostic tool and prognosis index in EL4-based T-ALL. Future studies of autofluorescence and the expression of CD25 should be broadened to research the underlying mechanism of the changes, regulations and biological characteristics of CD25 expression, in which we can collect extensive information to address the clinical application of potential treatments for T-ALL.

Acknowledgment

Funding availability

This work was supported by National Natural Science Foundation of China (81770149), National Natural Science Foundation of China (81100350).

Contributions of Authors

Zhonghua Du: designed and performed experiments, analyzed data, and drafted the manuscript; Lixia Wang: performed experiments and analyzed data; Yongguang Yang: contributed to the development of the project and edited the manuscript; Yanping Yang: conceived the research project, designed experiments, analyzed data, and wrote the paper.

References

1. Chiaretti S, Foà R (2009) T-cell acute lymphoblastic leukemia. Haematologica 94: 160-2.

2. Georgakoudi I, Jacobson BC, Müller MG, Sheets EE, Badizadegan K, et al. (2002) NAD(P)H and collagen as in vivo quantitative fluorescent biomarkers of epithelial precancerous changes. Cancer Res 62: 682-7.

3. Zhang J, Wu J, Yang Y, Liao H, Xu Z, et al. (2016) White light, autofluorescence and narrow-band imaging bronchoscopy for diagnosing airway pre-cancerous and early cancer lesions: a systematic review and meta-analysis. J Thorac Dis 8: 3205-16.

4. Shah AT, Diggins KE, Walsh AJ, Irish JM, Skala MC (2015) In Vivo Autofluorescence Imaging of Tumor Heterogeneity in Response to Treatment. Neoplasia 17: 862-70.

5. Rehman AU, Anwer AG, Gosnell ME, Mahbub SB, Liu G, et al. (2017) Fluorescence quenching of free and bound NADH in HeLa cells determined by hyperspectral imaging and unmixing of cell autofluorescence. Biomed Opt Express 8: 1488-98.

6. Pantanelli SM, Li Z, Fariss R, Mahesh SP, Liu B, et al. (2009) Differentiation of malignant B-lymphoma cells from normal and activated T-cell populations by their intrinsic autofluorescence. Cancer Res 69: 4911-7.

7. Takeuchi Y, Hanaoka N, Hanafusa M, Ishihara R, Higashino K, et al. (2011) Autofluorescence imaging of early colorectal cancer. J Biophotonics 4: 490-7.

8. Ragunath K (2007) Autofluorescence endoscopy--not much gain after all? Endoscopy 39: 1021-2.

9. Yu Q, Heikal AA (2009) Two-photon autofluorescence dynamics imaging reveals sensitivity of intracellular NADH concentration and conformation to cell physiology at the single-cell level. J Photochem Photobiol B 95: 46-57.

10. Xu RH, Pelicano H, Zhou Y, Carew JS, Feng L, et al. (2005) Inhibition of glycolysis in cancer cells: a novel strategy to overcome drug resistance associated with mitochondrial respiratory defect and hypoxia. Cancer Res 65: 613-21.

11. Pavlova I, Sokolov K, Drezek R, Malpica A, Follen M, et al. (2003) Microanatomical and biochemical origins of normal and precancerous cervical autofluorescence using laser-scanning fluorescence confocal microscopy. Photochem Photobiol 77: 550-5.

12. Blacker TS, Duchen MR (2016) Investigating mitochondrial redox state using NADH and NADPH autofluorescence. Free Radic Biol Med 100: 53-65.

13. Nadhi T, Sharmila A, Rebecca RK (2011) Optical molecular imaging for detection of Barrett's-associated neoplasia. World J Gastroenterol 17: 53-62.

14. Bird DK, Yan L, Vrotsos KM, Eliceiri KW, Vaughan EM, et al. (2005) Metabolic mapping of MCF 10A human breast cells via multiphoton fluorescence lifetime imaging of the coenzyme NADH. Cancer Res 65: 8766-73.

15. Modica NJS, Singh KK (2004) Mitochondrial dysfunction in cancer. Mitochondrion 4: 755-62.

16. Shah AT, Cannon TM, Higginbotham JN, Coffey RJ, Skala MC (2017) Autofluorescence flow sorting of breast cancer cell metabolism. J Biophotonics 10: 1026-33.

17. Heintzelman DL, Lotan R, Richards KRR (2000) Characterization of the autofluorescence of polymorphonuclear leukocytes, mononuclear leukocytes and cervical epithelial cancer cells for improved spectroscopic discrimination of inflammation from dysplasia. Photochem photobiol 71: 327-32.

18. Schuh K, Twardzik T, Kneitz B, Heyer J, Schimpl A, et al. (1998) The interleukin 2 receptor alpha chain/CD25 promoter is a target for nuclear factor of activated T cells. J Exp Med 188: 1369-73.

19. Sullivan RP, Leong JW, Schneider SE, Ireland AR, Berrien-Elliott MM, et al. (2015) MicroRNA-15/16 Antagonizes Myb To Control NK Cell Maturation. J Immunol 195: 2806-17.

20. Meunier MC, Roy-Proulx G, Labrecque N, Perreault C (2003) Tissue distribution of target antigen has a decisive influence on the outcome of adoptive cancer immunotherapy. Blood 101: 766-70.

21. Ashfaq K, Yahaya I, Hyde C, Andronis L, Barton P, et al. (2010) Clinical effectiveness and cost-effectiveness of stem cell transplantation in the management of acute leukaemia: a systematic review. Health Technol Assess 14: 1-141.

22. Kumar P, Rao S, Kamath SD, Prabhu V, Satyamoorthy K, et al. (2011) Autofluorescence of Osteoporotic Mouse Femur Bones:A Pilot Study. Photomed Laser Surg 29: 227-32.

23. Ramanujam N (2000) Fluorescence spectroscopy of neoplastic and non-neoplastic tissues. Neoplasia 2: 89-117.

24. Kamath SD, Bhat RA, Ray S, Mahato KK (2009) Autofluorescence of normal, benign, and malignant ovarian tissues: a pilot study. Photomed Laser Surg 27: 325-35.

25. Ueno N, Fujiya M, Moriichi K, Ikuta K, Nata T, et al. (2011) Endosopic Autofluorescence Imaging is Useful for the Differential Diagnosis of Intestinal Lymphomas Resembling Lymphoid Hyperplasia. J Clin Gastroenterol 45: 507-13.

26. Riew TR, Kim HL, Choi JH, Jin X, Shin YJ, et al. (2017) Progressive accumulation of autofluorescent granules in macrophages in rat striatum after systemic 3-nitropropionic acid: a correlative light- and electron-microscopic study. Histochem Cell Biol 148: 517-28.

27. Chen J, Zhang M, Ju W, Waldmann TA (2009) Effective treatment of a murine model of adult T-cell leukemia using depsipeptide and its combination with unmodified daclizumab directed toward CD25. Blood 113: 1287-93.

28. Monici M, Agati G, Fusi F, Pratesi R, Paglierani M, et al. (2003) Dependence of leukemic cell autofluorescence patterns on the degree of differentiation. Photochem Photobiol Sci 2: 981-7.

29. Pui CH, Robison LL, Look AT (2008) Acute lymphoblastic leukaemia. Lancet 371:1030-43.

Submit your next manuscript to Annex Publishers and benefit from:

- Easy online submission process
- Rapid peer review process
- Online article availability soon after acceptance for Publication
- Open access: articles available free online
- More accessibility of the articles to the readers/researchers within the field
- Better discount on subsequent article submission

Submit your manuscript at
http://www.annexpublishers.com/paper-submission.php